NOVEL FLAT-PLATE SOLAR COLLECTOR WITH AN INCLINED N-S AXIS AND RELATIVE E-W TRACKING ABSORBERS AND THE NUMERICAL ANALYSIS OF ITS POTENTIALS

by

Aleksandar M. NEŠOVIĆ[a], Nebojša S. LUKIĆ[b], Mladen M. JOSIJEVIĆ[b*], Nebojša M. JURIŠEVIĆ[b], and Novak N. NIKOLIĆ[b]

[a] Institute for Information Technologies, University of Kragujevac, Kragujevac, Serbia
[b] Faculty of Engineering, University of Kragujevac, Kragujevac, Serbia

Original scientific paper
https://doi.org/10.2298/TSCI230201115N

The current flat-plate solar collectors perform best when their absorbers rotate around their axis. However, with their concentrators, reflectors, and tracking mechanisms, they take up a lot of space and are thus commercially speaking, not the best solutions. This paper proposes a novel solar collector design which employs the (relative) rotation of absorbers, but strives to combine the benefits of fixed and (absolute) tracking solar systems, i.e. volume occupancy from the former and thermal performance from the latter. The findings of our numerical analysis show that, the solar irradiance efficiency of this novel design is 20% higher than that of a fixed flat-plate collector during clear-sky days, and it is equally lower than that of an absolute tracking collector. This paper also introduces a new criterion for describing single-axis tracking solar collectors which should be included in the classifications of solar collectors. Finally, the article, which represents a continuation of our research in the field of solar energy utilization, can contribute to the future development of solar technologies and solve some of the current challenges.

Key words: *EnergyPlus software, fixed solar system, flat-plate solar collector, novel solar design, dimulation, tracking solar system*

Introduction

Various types of solar collectors (SC) are present in the international market. Diverse SC with different designs of their integral components differ in their production costs, volume occupancies (VO), and thermal efficiency, which all further impact their availability and applicability. The literature them into two major categories: fixed and tracking (non-concentrating and concentrating) designs.

Due to their relatively good price/performance ratios, flat-plate (FP) SC, with [1] and without [2] circulation pumps, have found a widespread use in both residential and industrial sector [3-6], and have the largest share at the market. Their commercial success testifies to the fact that even minor reductions in VO, which would not alter efficiency/cost ratios of FP significantly, could enhance the practical application and utilization of solar energy.

When it comes to one-sided reflectors, the literature provides numerous solutions focused on improving thermal performances of FP. In 1970, an aluminum reflector was installed under an FP so it became a double-exposed system [7]. The innovation was quickly adopted and incorporated into the existent architectural concept of a housing unit. Similar variations of FP

* Corresponding author, e-mail: mladenjosijevic@gmail.com

and one-side reflectors have been tested in various geographical locations [8-14]. In terms of their properties, these constructions can be classified as both active and passive solar systems.

There are also numerous examples of FP with double-side reflectors, upper and lower [15], left and right [16], and multi-side reflectors, three-sided [17], and four-sided [18]. Baccoli *et al*. [19, 20] first created a mathematical model of an FP with a lower reflector and then they provided a comprehensive optimization model. Nikolić and Lukić [21, 22] placed a manually-moving reflector in all three orthogonal directions parallel and under an FP. Theoretical and experimental studies on the performances of these constructions with double-exposed FP revealed that the thermal performance of a conventional FP can be improved by 29.55%. Another relatively interesting experimental study was conducted in Iraq by Abd *et al*. [23]. The study proposed an SC system with a compound parabolic concentrator (CPC) behind an FP receiver and their solution exhibited better thermal performances than the conventional FP by 26.5% .

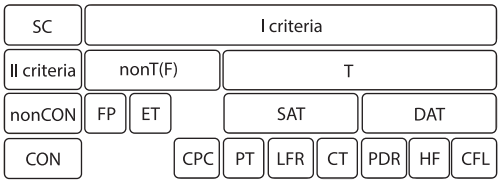

Figure 1. Traditional SC classifications [24-27]: *nonCON – non-concentrating, CON – concentrating, nonT – non-tracking (fixed), T – tracking, ET – evacuated tube, SAT – single-axis tracking, DAT – dual-axis tracking, PT – parabolic trough, LFR – linear Fresnel lens, CT – cylindrical trough, PDR – parabolic dish reflectors, HF – heliostat fields, CFL – circular Fresnel lens*

According to the traditional classifications, FP are non-concentrating and non-tracking systems, fig. 1. The development of solar technology has demonstrated that this does not have to be so. The recent literature offers solutions in which FP are tracking systems. One such option (E-W tracking FP) was explored numerically by Neville [28]. Drago [29] investigated the possibility of a fully tracking FP numerically, and Attalage and Reddy [30] did something similar. In Brazil, Maia *et al*. [31] developed a mathematical model that demonstrated that a fully tracking FP is superior to a single-axis tracking FP. Finally, Hafez *et al*. [32] made a significant contribution in this field with their review article which provides a comprehensive overview of the investigated solutions in solar tracking technology.

Despite all the advances in terms of thermal efficiency, the aforementioned FP have one major drawback in common. The VO increases by even several times with respect to fixed FP due to additional equipment installations (reflectors and tracking systems). As a result, the indicator Q_{FP}/VO [Wm^{-3}] of such systems can make them less favorable in commercial terms. Solar tracking designs which can increase thermal efficiency without an additional increase in VO may prove to be more favorable. Thus, they can find wide-spread application and consequently, increase the general utilization of solar energy.

One such system is proposed in this article – a SC-type FP with an inclined N-S axis and relative E-W tracking absorbers (IrSATA). This novel design was invented aiming at overcoming the challenges of high VO present in advanced IFA designs (an FP with inclined and fixed absorbers). The performances of the IrSATA were numerically tested in the EnergyPlus software package. The assessments should indicate whether it is viable to invest any efforts into the construction of this system and into the practical experiments.

EnergyPlus software lacks a platform for studying solar tracking systems so it was used here in step-by-step modelling. The methodology of this article offers special contributions in that it proposes novel possibilities of utilizing this software solution.

Since the novel concept design proposed in this paper does not fully fit into the current SAT classification, we will advocate for the introduction of two additional criteria: active (aSAT) and relative (rSAT).

Materials and methods

Model description

Traditional and advanced IFA designs are presented in fig. 2. The novel design is given in fig. 2(b). The common (central) mechanism that simultaneously rotates each absorber plate (in the same direction and with the same rotation step) enables smaller VO. The design allows the collector to outperform the simple IFA design's, fig. 2(a), in terms of thermal efficiency while adding negligible VO, which is smaller than with other designs presented in fig. 2(c)-2(i). For this to be possible, the proposed model design allows for the relative (internal) movement of the SC components while the whole structure has no (external) movements.

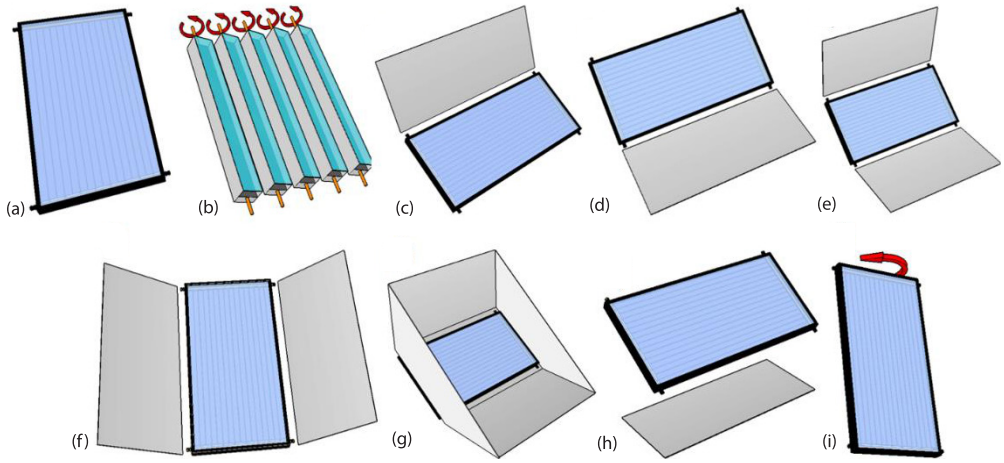

Figure 2. Traditional and novel FP designs; (a) IFA [33, 34], (b) IrSATA, (c) IFA with behind reflector [8-13], (d) IFA with front reflector [8-13], (e) IFA with front and behind reflectors [15], (f) IFA with side reflectors [15], (g) IFA with multi-side reflectors [35], (h) IFA with bottom reflector [21, 22], and (i) IaSATA

Solar irradiance

An EnergyPlus solar irradiance model is illustrated in fig. 3. The event's model calculation is relatively complicated. However, it can be represented in a briefer form as the sum of the beam, I_B [Wm^{-2}], diffuse, I_D [Wm^{-2}], and reflected, I_R [Wm^{-2}] solar radiation [36]:

$$I_{TOT} = I_B + I_D + I_R \tag{1}$$

where I_{TOT} [Wm^{-2}] is the total incident solar radiation on FP surface.

Diffuse solar radiation originates from the circumsolar region, $I_{D\text{-}CIR}$ [Wm^{-2}], sky dome, $I_{D\text{-}SD}$ [Wm^{-2}], and sky horizon, $I_{D\text{-}SH}$ [Wm^{-2}]:

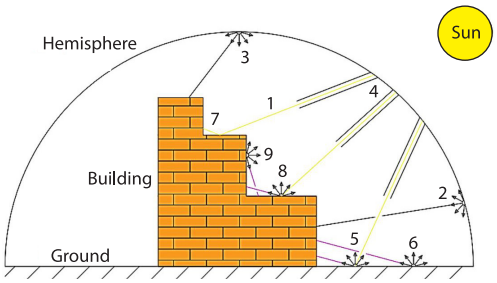

Figure 3. Solar irradiance model: *1 – I_B, 2 – $I_{D\text{-}SH}$, 3 – $I_{D\text{-}SD}$, 4 – $I_{D\text{-}CIR}$, 5 – $I_{R\text{-}G(BtoD)}$, 6 – $I_{R\text{-}G(D)}$, 7 – $I_{R\text{-}O(BoB)}$, 8 – $I_{R\text{-}O(BtoD)}$, and 9 – $I_{R\text{-}O(D)}$*

$$I_D = I_{D\text{-}CIR} + I_{D\text{-}SD} + I_{D\text{-}SH} \tag{2}$$

The reflection of the Sun's rays from the ground, $I_{R\text{-}G}$ [Wm^{-2}], eq. (4) and other obstacles, $I_{R\text{-}O}$ [Wm^{-2}], eq. (5) lead to reflected solar radiation:

$$I_{\mathrm{R}} = I_{\mathrm{R\text{-}G}} + I_{\mathrm{R\text{-}O}} \tag{3}$$

$$I_{\mathrm{R\text{-}G}} = I_{\mathrm{R\text{-}G(BtoD)}} + I_{\mathrm{R\text{-}G(D)}} \tag{4}$$

$$I_{\mathrm{R\text{-}O}} = I_{\mathrm{R\text{-}O(BtoB)}} + I_{\mathrm{R\text{-}O(BtoD)}} + I_{\mathrm{R\text{-}O(D)}} \tag{5}$$

where $I_{\mathrm{R\text{-}G(BtoD)}}$ [Wm^{-2}] is the beam-to-diffuse solar radiation reflected from the ground, $I_{\mathrm{R\text{-}G(D)}}$ [Wm^{-2}] – the diffuse solar radiation reflected from the ground, $I_{\mathrm{R\text{-}O(BtoB)}}$ [Wm^{-2}] – the beam-to-beam solar radiation reflected from the obstacles, $I_{\mathrm{R\text{-}O(BtoD)}}$ [Wm^{-2}] – the beam-to-diffuse solar radiation reflected from the obstacles, and $I_{\mathrm{R\text{-}O(D)}}$ [Wm^{-2}] is diffuse solar radiation reflected from the obstacles.

Thermal performance

EnergyPlus software has an integrated simple model for determining the FP thermal efficiency, (η_{FP} [–], which is based on the application of quadratic correlation [36]:

$$\eta_{\mathrm{FP}} = c_0 + c_1 \frac{T_{\mathrm{w\text{-}in}} - T_{\mathrm{air}}}{I_{\mathrm{TOT}}} + c_2 \frac{\left(T_{\mathrm{w\text{-}in}} - T_{\mathrm{air}}\right)^2}{I_{\mathrm{TOT}}} \tag{6}$$

where c_0, c_1, and c_2 [–] are the correction factors, $T_{\mathrm{w\text{-}in}}$ [K] – the water inlet absolute temperature, and T_{air} [K] – the absolute temperature of the ambient air.

The FP heat power, Q_{FP} [W], eq. (7) and water outlet absolute temperature, $T_{\mathrm{w\text{-}out}}$ [K], eq. (8) [36]:

$$Q_{\mathrm{FP}} = \eta_{\mathrm{FP}} Q_{\mathrm{SUN}} = \eta_{\mathrm{FP}} A_{\mathrm{FP}} I_{\mathrm{TOT}} \tag{7}$$

$$T_{\mathrm{w\text{-}out}} = \frac{Q_{\mathrm{FP}}}{\dot{m}_{\mathrm{w}} c_p} + T_{\mathrm{w\text{-}in}} \tag{8}$$

where Q_{SUN} [W] is the solar heat power (heat flux), A_{FP} [m^2] – the absorber area, $\dot{m}_{\mathrm{w}}$ [kgs^{-1}] – the mass-flow rate, and c_p [Jkg^{-1}K^{-1}] – the specific heat.

Meteorological data

Average (EneryPlus) daily values of the beam and diffuse solar radiation on a horizontal surface (from June 15 to October 15), for the city of Kragujevac, are presented in fig. 4. The same diagram shows the average daily air temperature during the same period.

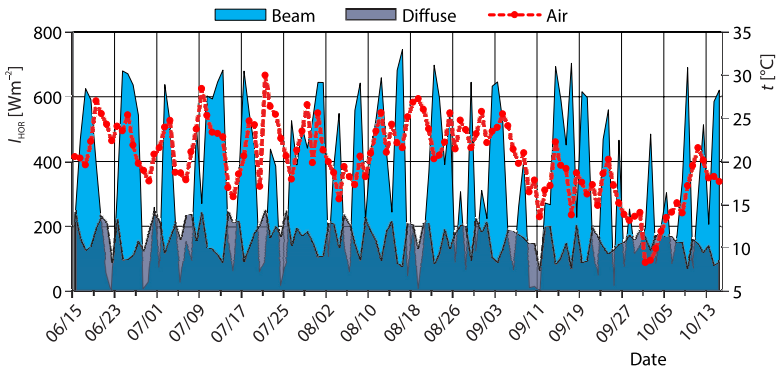

Figure 4. Meteorological data for the city of Kragujevac

Simulation scenario

Three FP models were designed to meet the numerical requirements of the study, fig. 5:

– *Scenario S1*. The FP with inclined N-S axis and fixed absorbers (IFA).
– *Scenario S2*. The FP with inclined N-S axis and absolute E-W tracking absorbers (IaSATA).
– *Scenario S3*. The FP with inclined N-S axis and relative E-W tracking absorbers (IrSATA).

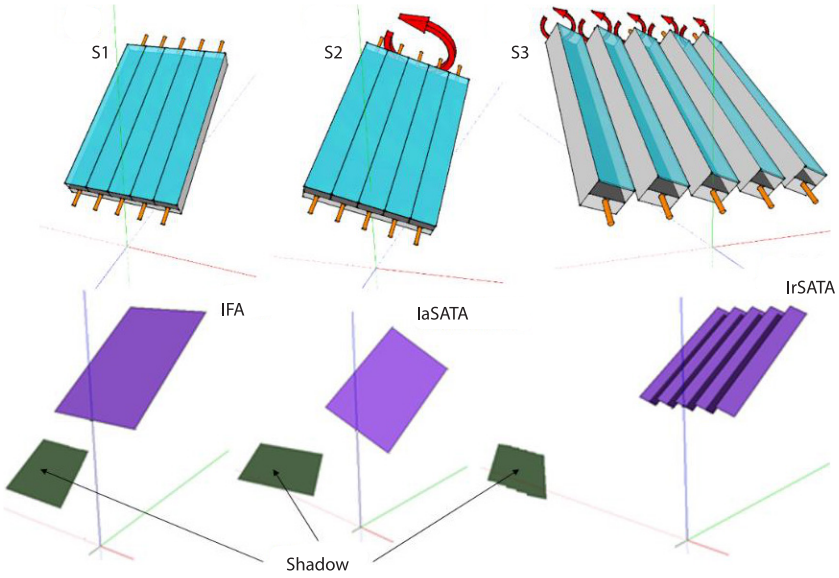

Figure 5. Scenario simulation

The FP geometries are defined in the Google SketchUp software package by using a relatively novel EnergyPlus Shading Group tool from the Legacy OpenStudio plugin. All of the models used in the study had the same system dimensions (ASO = 0.4 m^2). Accordingly, the IrSATA was comprised of five absorbers with dimensions of 800 mm × 100 mm. A more detailed description of the models is presented in tab. 1.

Because the EnergyPlus software lacks models for IaSATA and IrSATA application simulations, they are performed step-by-step here. The daily amount of solar energy that falls on IaSATA and IrSATA was determined through a series of simulations for each minute during the day (software limit) and for each angle of the absorber rotation: –90° (sunrise time) to +90° (sunset time). Simulations were performed from June 15 to October 15. The sample size was sufficient to show how FP behave at various intensities of solar irradiance, and thus at various ratios of the beam and diffuse solar radiation.

Results and discussion

The average daily heat powers for IFA, IrSATA, and IaSATA during the analyzed period (from June 15th to October 15th) are shown in fig. 6.

The average daily heat powers of the analyzed FP (IFA, IrSATA, IaSATA) during the whole period were, fig. 6: 83.13 W, 95.95 W, and 114.1 W, respectively. It can be concluded that IrSATA heat power was 15.43% higher than IFA heat power. The IaSATA heat power was 37.26% higher than IFA and 18.92% higher than IrSATA.

The highest average daily heat power for IFA was 139.58 W (August 12th, fig. 6). On that day, IrSATA heat power was 163.47 W, and IaSATA 192.61 W. On the other hand, the

Table 1. The FP geometric characteristics

Scenario	Unit	S1	S2	S3
FP	–	IFA	IaSATA	IrSATA
Inclined angle	[°]	34 [37]		
Absorbers number	[–]	5		
Total absorber width	[mm]	500		600
Total absorber length	[mm]	800		
One absorber plate width	[mm]	100		
Ground vertical distance	[mm]	700		
ASO	[m^2]	0.4		
TSO	[m^2]	0.4		0.48
VO	[m^3]	–	0.157	0.0314
Simulation number	[–]	–	181	
Location	–	Kragujevac, Serbia		
Run period	–	From June 15th to October 15th		
Water inlet temperature	[°C]	30		
Water mass-flow rate	[kgs^{-1}]	0.006 (0.015 kg/sm^2 [2])		

lowest heat powers of the FP were recorded on June 22nd (I_{TOT} = 89.59 W/m^2, figs. 4 and 6: 6.63 W (for IFA), 6.66 W (for IrSATA), and 6.7 W (for IaSATA). During unfavorable weather conditions (*e.g.* September 11th, I_{TOT} < 70 W/m^2, t_{air} = 14 °C, fig. 4), FP cannot be used due to their technical requirements ($t_{w\text{-}in}$ = 30 °C, $\dot{m}_w$ = 0.006 kg/s) from tab. 1.

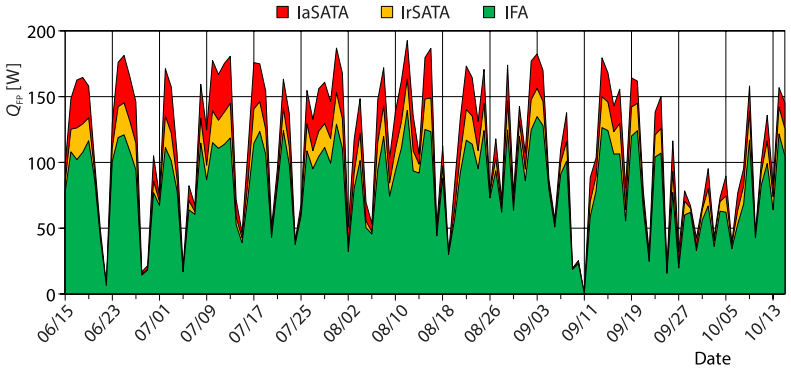

Figure 6. The IFA, IrSATA, and IaSATA average daily heat powers

Because IFA does not have a tracking mechanism, the solar incident angle [38], formed by the vector normal to the FP surface and the Sun rays (its beam component), changes during the day. Unlike IFA, the IaSATA surface in the transverse plane is normal to the direction of the Sun rays during the day, which is why this FP has the highest solar potential. The IrSATA solar potential (although it has a tracking mechanism) is reduced due to solar shading, which occurs as a result of the relative rotation of the absorbers within the complete solar structure.

When the share of beam solar radiation in the total solar radiation decreases, FP begin to behave identically because diffuse solar radiation from all directions reaches their surfaces in nearly equal amounts.

For better understanding, we shall present the data for one randomly selected clear-sky date (July 26th). Figure 7 shows meteorological data and fig. 8 shows FP heat powers.

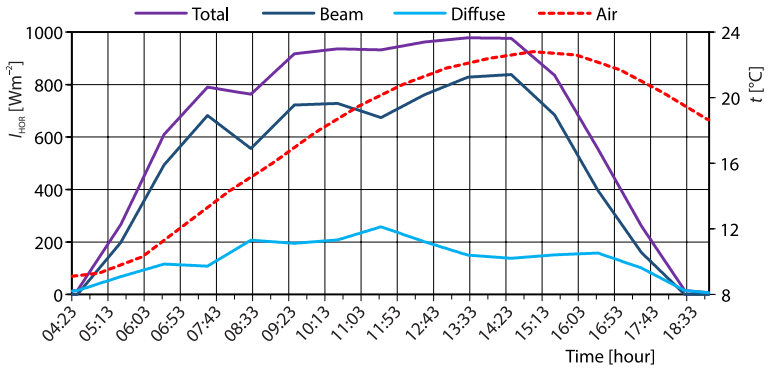

Figure 7. Meteorological data (July 26th)

Although the Sun rose at 04:23 a. m. and set at 19:03 p. m. (on July 26th), the IFA can use solar energy during the time period from 06:49 a. m. to 17:14 p. m. The reasons for this include: technical requirements, tab. 1, the solar radiation intensity (which is much lower in the morning and evening, fig. 7), and the solar incident angle.

By applying the aSATA mechanism on the IFA (IaSATA), the solar incidence angle is *modified* by increasing the incoming solar radiation on this tracking FP. Thanks to this advantage, the intensity of solar radiation was increased by many times in the morning and evening hours, which allows for extended working time of IaSATA, fig. 8, for 74 minutes in the morning (starting at 05:35 a. m.) and 44 minutes in the evening (stop at 17:58 p. m.). Due to the shading effect, IrSATA could operate from 06:23 a. m. to 17:25 p. m. on July 26th, fig. 8 – start and stop are *between* the daily operating hours of IFA and IaSATA.

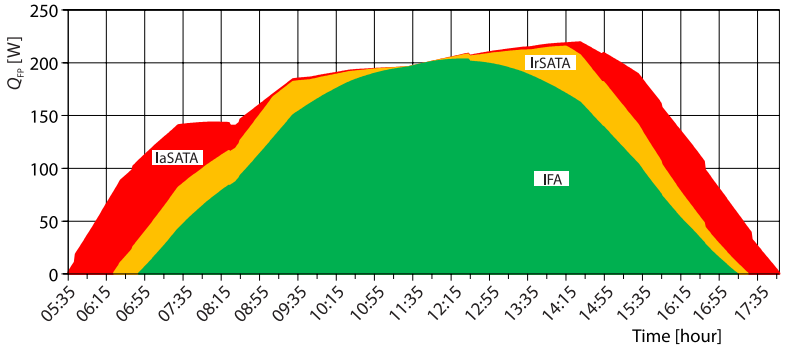

Figure 8. Heat powers comparisons for different FP types (July 26th)

Figure 8 demonstrates that for a short period, all three types of FP have equal heat powers, which in this case was 198.49 W (on July 26th). The equilibrium occurs at the moment when the Sun reaches its daily zenith position (the moment of solar noon, 11:43 a, m.). Then all absorber plates (valid for all three FP types) occupy the same position, *i.e.* the same parallel plane with the same angle and the same height to the horizontal surface.

It should also be noted that solar radiation was most intense at 13:30 p. m. ($I_{HOR\text{-}TOT}$ = 978 W, fig. 7), but that due to the specific tracking systems, all FP reached the highest heat power at certain times, fig. 8: IFA (203.2 W, 12:30 p. m.), IrSATA (215.3 W,

14:15 p.m.), and IaSATA (219.39 W, 14:30 p. m.). The studied FP heat powers correspond to the following water outlet temperatures of the FP: 8.09 °C (IFA, 12:30 p. m.), 8.57 °C (IrSATA, 14:15 p. m.), and 8.73 °C (IaSATA, 14:30 p. m.).

Although the simulation results for the analyzed period show that IaSATA had the highest heat power, fig. 6, the situation changed when the indicators ASO, TSO, and VO are taken into consideration, which is confirmed by tab. 2.

Table 2. Comparison of the SC using different indicators (July 26th)

FP	Q_{FP} [W]	Q_{FP}/ASO [Wm^{-2}]	Q_{FP}/TSO [Wm^{-2}]	Q_{FP}/VO [Wm^{-3}]
IFA	108.77	271.93		–
IrSATA	129.33	323.34	269.45	4118.94
IaSATA	154.66	386.64		985.07

If IrSATA and IaSATA are compared considering the Q_{FP}/TSO indicator, the differences are even greater (for 46.76%, July 26th) in favor of IaSATA. According to this indicator, IFA can have better performance than IrSATA in some circumstances, tab. 2. However, the Q_{FP}/VO ratio of IrSATA is far better (×4.18) than IaSATA. As a result, the novel design makes the collector system more compact and suitable for practical applications.

Despite a number of advantages, the eventual physical realization of the new idea concept (IrSATA) in the future would be accompanied by the following technical problems:

– Selection of a power unit.
– Selection of the place for the installation of the power unit.
– Selection of electro-mechanical transmission.
– Connection of stationary (splitter and mixer) and moving (absorber plates) elements.
– Sun tracking method – date and time, electro-optical sensors, a combination of the first two [39].
– Designing suitable supports for stationary and moving elements, *etc.*

Further classification of the solar tracking systems

The concept of Sun tracking absorbers that can rotate around their axis is novel in the field of applied solar technology. Figure 9 uses sets to graphically represent the classification of SAT before (left) and after (right) the division supplementation by IrSATA. The traditional classification considered two criteria [39-44]: the axis of rotation (horizontal, inclined, or vertical) and the rotational direction (E-W tracking, N-S tracking). The E-W tracking system is compatible with all types of axes of rotation, whereas the N-S tracking system is unique to the horizontal axis of rotation.

In addition the two previously mentioned criteria, this study supplements the third classification criterion – the method of rotating SAT (absolute or external tracking, and relative or internal tracking).

In the first case, the absorbers are always in the same (common) plane. At rest, they are relative to one another, tracking the Sun as a whole and receiving the same amount of solar energy. In the second case, the mutual position of the absorbers changes over time (they are only in the same plane at solar noon), while the absorbers share a rotation mechanism (all absorbers rotate at the same angular speed and in the same direction). Except for the end absorbers, they all receive the same amount of solar radiation reduced by the shaded portion, which is determined by their mutual axial distance.

The first type of SAT requires a large amount of space to provide adequate working conditions, whereas the second type is nearly identical to the IFA.

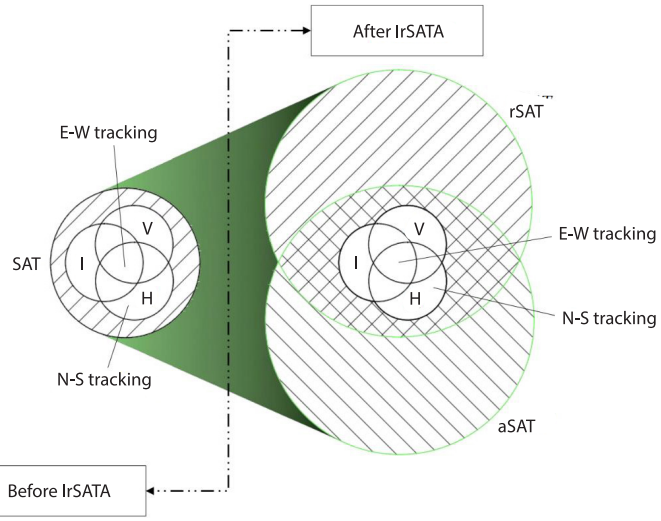

Figure 9. The SAT advanced classification

Considering the third criterion for the SAT classification, the existing classification can be applied to both aSAT and rSAT, which mathematically can be described as the intersection of the aSAT and rSAT sets, fig. 9.

Conclusions

This paper analyses the potentials of the novel design, *i.e.* an FP with an inclined N-S axis and relative E-W tracking absorbers (IrSATA). The novel design's potentials were compared to other commonly used designs in the literature, namely IaSATA and IFA.

The numerical analyses were performed in the EnergyPlus software package. Because the software does not include any existing models for analyzing such a design, the models were created step-by-step, making a significant contribution in terms of software utilization possibilities.

The new IrSATA design has roughly the same VO as IFA, which is a relatively significant indicator that it has usually been overlooked by scientists engaged in the advancement of FP. Aside from that, the novel design incorporates a tracking system similar to IaSATA. Because of the relative rotation of the absorbers, the new FP design can gather up to 20% more solar energy than IFA on clear-sky days.

As a result, the novel IrSATA design achieves the optimal balance between IFA and IaSATA systems, combining the advantages of both: VO from the former and heat power from the latter. The novel system, therefore, enables the use of relatively efficient collectors that have no impact on the spatial and aesthetic components of the buildings that house them.

Because the provided collector design utilizes an unusual tracking system, an adjustment to the standard SAT classification has been proposed, while the category of *rotating SAT* has been introduced to the traditional classification catalog.

Acknowledgment

This investigation is a part of project TR 33015 of the Technological Development of the Republic of Serbia. We would like to thank the Ministry of Education, Science and Technological Development of the Republic of Serbia for their financial support during this investigation.

Nomenclature

A – area, [m^2]
c_0, c_1, c_2 – correction factors, [–]
c_p – specific heat, [Jkg^{-1}K^{-1}]
I – solar radiation, [W]
$\dot{m}$ – mass-flow rate, [kgs^{-1}]
Q – heat power, [W]
T – absolute temperature, [K]

Greek letter

η – efficiency, [–]

Subscripts

air – air
B – beam
CIR – circumsolar region
D – diffuse
G – ground
HOR– horizontal
in – inlet
O – obstacle
out – outlet
R – reflection
SD – sky dome
SH – sky horizon
SUN – solar
TOT – total
w – water

Acronyms

a – absolute
ASO – active surface occupancy
CFL – circular Fresnel lens
CON – concentrating
CPC – compound parabolic concentrator
CT – cylindrical trough
DAT – dual-axis tracking
ET – evacuated tube
FP – flat-plate
H – horizontal (axis)
HF – heliostat fields
I – inclined (axis)
IaSATA – FP with inclined and absolute SAT absorbers
IFA – FP with inclined and fixed absorbers
IrSATA – FP with inclined and relative SAT absorbers
LFR – linear Fresnel lens
nonCON – non-concentrating
nonT – non-tracking (fixed)
PDR – parabolic dish reflectors
PT – parabolic trough
r – relative
SAT – single-axis tracking
SC – solar collector
T – tracking
TSO – total surface occupancy
V – vertical (axis)
VO – volume occupancy

References

[1] Noghrehabadi, A., *et al*., An Experimental Study of the Thermal Performance of the Square and Rhombic Solar Collectors, *Thermal Science*, *22* (2018), 1, pp. 487-494
[2] Nešović, A., *et al*., Experimental Analysis of the Fixed Flat-Plate Solar Collector with Sn-Al_2O_3 Selective Absorber and Gravity Water Flow, *Thermal Science*, *27* (2023), 1A, pp. 349-358
[3] Khalifa, A. J. N., Thermal Performance of Locally Made Flat Plate Solar Collectors Used as Part of a Domestic Hot Water System, *Energy Convers. Manag*., *40* (1999), 17, pp. 1825-1833
[4] Tiwari, A. K., *et al*., The TRNSYS Simulation of Flat Plate Solar Collector Based Water Heating System in Indian Climatic Condition, *Mater. Today Proc*., *46* (2021), 11, pp. 5360-536
[5] Moss, R.W., *et al*., Simulator Testing of Evacuated Flat Plate Solar Collectors for Industrial Heat and Building Integration, *Sol. Energy*, *164* (2018), Apr., pp. 109-118
[6] Atmaca, I., Kocak, S., Theoretical Energy and Exergy Analyses of Solar Assisted Heat Pump Space Heating System, *Thermal Science*, *18* (2014), Suppl. 2, pp. S417-427
[7] Safwat, H. H., Souka, A. F., Design of a New Solar-Heated House Using Double-Exposure Flat-Plate Collectors, *Sol. Energy*, *13* (1970), 1, pp. 105-119
[8] Grassie, S. L., Sheridan, N. R., The Use of Planar Reflectors for Increasing the Energy Yield of Flat-Plate Collectors, *Sol. Energy*, *19* (1977), 6, pp. 663-668
[9] Taha, I. S., Eldighidy, S. M., Effect of Off-South Orientation on Optimum Conditions for Maximum Solar Energy Absorbed by Flat Plate Collector Augmented by Plane Reflector, *Sol. Energy*, *25* (1980), 4, pp. 373-379
[10] Chiam, H. F., Stationary Reflector-Augmented Flat-Plate Collectors, *Sol. Energy*, *29* (1982), 1, pp. 65-69
[11] Arata, A. A., Geddes, R. W., Combined Collector-Reflector Systems, *Energy*, *11* (1986), 6, pp. 621-630
[12] Bollentin, J. W., Wilk, R. D., Modelling the Solar Irradiation on Flat Plate Collectors Augmented with Planar Reflectors, *Sol. Energy*, *55* (1995), 5, pp. 343-354

[13] Qiu, G., *et a*l., Comparative Study on Solar Flat-Plate Collectors Coupled with Three Types of Reflectors not Requiring Solar Tracking for Space Heating, *Renew. Energy*, *169* (2021), May, pp. 104-116
[14] Tanaka, H., Theoretical Analysis of Solar Thermal Collector and Flat Plate Bottom Reflector with a Gap between Them, *Energy Reports*, *1* (2015), Nov., pp. 80-88
[15] Chiam, H. F., Planar Concentrators for Flat-Plate Solar Collectors, *Sol. Energy*, *26* (1981), 6, pp. 503-509
[16] Bhowmik, H., Amin, R., Efficiency Improvement of Flat Plate Solar Collector Using Reflector, *Energy Reports*, *3* (2017), Nov., pp. 119-123
[17] Cisse, E. H. I., *et al*., Experimental Investigation of Solar Chimney with Concentrated Collector (SCCC), *Case Stud. Therm. Eng*., *35* (2022), 101965
[18] Rachedi, M. Y., *et al*., A Novel Model for Optimizing Tilts of Four Reflectors on A Flat Plate Thermal Collector: Case Study in Ouargla Region, *Case Stud. Therm. Eng*., *32* (2022), 101872
[19] Baccoli, R., *et al.*, A Mathematical Model of a Solar Collector Augmented by a Flat Plate above Reflector: Optimum Inclination of Collector And Reflector, *Energy Procedia*, *81* (2015), Dec., pp. 205-214
[20] Baccoli, R., *et al*., A Comprehensive Optimization Model for Flat Solar Collector Coupled with a Flat Booster Bottom Reflector Based on An Exact Finite Length Simulation Model, *Energy Convers. Manag*., *164* (2018), May, pp. 482-507
[21] Nikolić, N., Lukić, N., A Mathematical Model for Determining the Optimal Reflector Position of a Double Exposure Flat-Plate Solar Collector, *Renew. Energy*, *51* (2013), Mar., pp. 292-301
[22] Nikolić, N., Lukić, N., Theoretical and Experimental Investigation of the Thermal Performance of a Double Exposure Flat-Plate Solar Collector, *Sol. Energy*, *119* (2015), Sept., pp. 100-113
[23] Maher Abd, H., *et al*., Experimental Study of Compound Parabolic Concentrator with Flat Plate Receiver, *Appl. Therm. Eng*., *166* (2020), 114678
[24] Tyagi, V. V., *et al*., Advancement in Solar Photovoltaic/Thermal (PV/T) Hybrid Collector Technology, *Renew. Sustain. Energy Rev*., *16* (2012), 3, pp. 1383-1398
[25] Bhalla, V., Tyagi, H., Parameters Influencing the Performance of Nanoparticles-Laden Fluid-Based Solar Thermal Collectors: A Review on Optical Properties, *Renew. Sustain. Energy Rev*., *84* (2018), Mar., pp. 12-42
[26] Ghritlahre, H. K., Prasad, R. K., Application of ANN Technique to Predict the Performance of Solar Collector Systems – A Review, *Renew. Sustain. Energy Rev*., *84* (2018), Mar., pp. 75-88
[27] Zayed, M. E., *et al*., Applications of Cascaded Phase Change Materials in Solar Water Collector Storage Tanks: A Review, *Sol. Energy Mater. Sol. Cells*, *199* (2019), Sept., pp. 24-49
[28] Neville, R. C., Solar Energy Collector Orientation and Tracking Mode, *20* (1977), l, pp. 7-11
[29] Drago, P., A Simulated Comparison of the Useful Energy Gain in aFixed and a Fully Tracking Flat Plate Collector, *Sol. Energy*, *20* (1978), 5, pp. 419-423
[30] Attalage, R. A., Reddy, T. A., Annual Collectible Energy of a Two-Axis Tracking Flat-Plate Solar Collector, *Sol. Energy*, *48* (1992), 3, pp. 151-155
[31] Maia, C. B., *et al*., Evaluation of a Tracking Flat-Plate Solar Collector in Brazil, *Appl. Therm. Eng*., *73* (2014), 1, pp. 953-962
[32] Hafez, A. Z., *et al*., Solar Tracking Systems: Technologies And Trackers Drive Types – A Review, *Renew. Sustain. Energy Rev*., *91* (2018), Aug., pp. 754-782
[33] Moravej, M., *et al*., Enhancing the Efficiency of a Symmetric Flat-Plate Solar Collector Via the Use of Rutile TiO_2-Water Nanofluids, *Sustain. Energy Technol. Assessments*, *40* (2020), 100783
[34] Kaur, S., *et al*., Utilization of Biodegradable Novel Insulating Materials for Developing Indigenous Solar Water Heater for Hill Climates, *Energy Sustain. Dev*., *67* (2022), Apr., pp. 21-28
[35] Larson, D. C., Mirror Enclosures For Double-Exposure Solar Collectors, *Sol. Energy*, *23* (1979), 6, pp. 517-524
[36] ***, Development Team, E., EnergyPlus Engineering Documentation, 2013
[37] Đurđević, D. Z., Perspectives and Assessments of Solar PV Power Engineering in the Republic of Serbia, *Renew. Sustain. Energy Rev*., *15* (2011), 5, pp. 2431-2446
[38] Nešović, A., Theoretical Model of Solar Incident Angle for an Optionally Oriented Fixed Flat Surface, *Tehnik*a, *77* (2022), 3, pp. 328-333
[39] Awasthi, A., *et al*., Review on Sun Tracking Technology in Solar PV System, *Energy Reports*, *6* (2020), Nov., pp. 392-405
[40] Seme, S., *et al*., Solar Photovoltaic Tracking Systems for Electricity Generation: A Review, *Energies*, *13* (2020), 16, pp. 1-24
[41] Alexandru, C., Pozna, C., Simulation of a Dual-Axis Solar Tracker for Improving the Performance of a Photovoltaic Panel – Part A: *Proc. Inst. Mech. Eng. J. Power Energy*, 224 (2010), 6, pp. 797-811

[42] Jeong, K., *et al*., A Prototype Design and Development of the Smart Photovoltaic System Blind Considering the Photovoltaic Panel, Tracking System, And Monitoring System, *Appl. Sci*., *7* (2017), 10, pp. 1-18
[43] AL-Rousan, N., *et al*., Advances in Solar Photovoltaic Tracking Systems: A Review, *Renew. Sustain. Energy Rev*., *82* (2018), 3, pp. 2548-2569
[44] Sheikholeslami, M., *et al*., Recent Progress on Flat Plate Solar Collectors and Photovoltaic Systems in the Presence of Nanofluid: *A Review, J. Clean. Prod*., *293* (2021), 126119

Paper submitted: February 1, 2023
Paper revised: February 21, 2023
Paper accepted: March 8, 2023